Available online at www.sciencedirect.com
SCIENCE DIRECT®
Carbohydrate Research xxx (2004) xxx–xxx
Carbohydrate RESEARCH

A Fourier-transform infrared spectroscopy study of sugar glasses

Willem F. Wolkers,[a,b,*] Ann E. Oliver,[a,b] Fern Tablin[a,c] and John H. Crowe[a,b]

[a]*Center for Biostabilization, University of California, Davis, CA 95616, USA*
[b]*Section of Molecular and Cellular Biology, University of California, Davis, CA 95616, USA*
[c]*Department of Anatomy, Physiology, and Cell Biology, University of California, Davis, CA 95616, USA*

Received 31 October 2003; accepted 26 January 2004

Abstract—Fourier-transform infrared spectroscopy (FTIR) was used to study the hydrogen-bonding interactions that take place in vitrified carbohydrates of different chain lengths. The band position of the OH stretching band (*v*OH) and the shift in band position as a function of temperature were determined from the FTIR spectra as indicators for the length and strength of intermolecular hydrogen bonds, respectively. Differential scanning calorimetry (DSC) was used to corroborate the FTIR studies and to measure the change in heat capacity (ΔC_p) that is associated with the glass transition. We found that with increasing T_g, the band position of *v*OH increases, the wavenumber–temperature coefficient of *v*OH in the glassy state, WTC_g, increases, whereas ΔC_p decreases. The positive correlation that was found between *v*OH and the glass transition temperature, T_g, indicates that the length of the hydrogen bonds increases with increasing T_g. The increase in WTC_g with increasing T_g indicates that the average strength of hydrogen bonding decreases with increasing T_g. This implies that oligo- and polysaccharides (high T_g) have a greater degree of freedom to rearrange hydrogen bonds during temperature changes than monosaccharides (low T_g). Interestingly, WTC_g and ΔC_p showed a negative linear correlation, indicating that the change in heat capacity during the glass transition is associated with the strength of the hydrogen-bonding network in the glassy state. Furthermore, we report that introduction of poly-L-lysine in glassy sugar matrices decreases the average length of hydrogen bonds, irrespective of the size of the carbohydrate. Palmitoyl–oleoyl-phosphatidylcholine (POPC) vesicles were found to only interact with small sugars and not with dextran.
© 2004 Elsevier Ltd. All rights reserved.

Keywords: Carbohydrates; DSC; Desiccation tolerance; FTIR; Glasses; Trehalose

1. Introduction

Disaccharides such as trehalose and sucrose are found in high concentrations in organisms that naturally survive drying, where these compounds are thought to convey protection to intracellular biomolecules and organelles in the dried state. Trehalose is found in yeast, tardigrades, and brine shrimp,[1] whereas sucrose, in combination with oligosaccharides, is often found in seeds capable of surviving drying.[2] The stabilizing properties of these molecules in nature have found widespread application in the preservation of fragile biological materials. When freeze-drying is used as the method of drying, disaccharides can act as compatible solutes during freezing,[3] replace hydrogen bonds of biomolecules with water during drying, and form a glassy (amorphous) state with a high T_g in the dried state.[4] Sugars are able to inhibit fusion and to prevent leakage through the bilayer of unilamellar vesicles,[5] and they prevent conformational changes of proteins during drying.[6] Recently, sugars, particularly trehalose, have been implicated as protective agents to preserve mammalian cells by freeze-drying.[7–9]

In the amorphous state, carbohydrates form a fluid, solid-like matrix with a high viscosity and low molecular mobility, which is characterized by the glass transition temperature, T_g. The transition from the glassy to the rubbery state is a kinetic transition that can be measured as: (1) a change in heat capacity, using DSC;[10] (2) a drastic increase in rotational mobility, using electron paramagnetic resonance,[11] NMR spectroscopy,[12] or

* Corresponding author. Tel.: +1-530-752-1094; fax: +1-530-752-5305; e-mail: wolkers@yahoo.com

0008-6215/$ - see front matter © 2004 Elsevier Ltd. All rights reserved.
doi:10.1016/j.carres.2004.01.016

optical luminescence;[13] or (3) an abrupt change in hydrogen bonding, using Fourier-transform infrared spectroscopy (FTIR).[14] The main advantages of the latter technique are that it reveals information at the molecular level and that it does not require incorporation of probe molecules. The main experimental parameter that can be derived from infrared spectra is the band position of characteristic molecular group vibrations. In addition, the thermotropic response of the IR absorption bands can in some cases be used to detect phase transitions of the system. The glass transition of carbohydrates can be measured as an abrupt change in the wavenumber–temperature coefficient (*WTC*) of the OH stretching band arising from the sugar OH groups, located between 3600 and 3000 cm^{-1}.[14] The *WTC* is a measure of the change in hydrogen-bond strength with the temperature in the system.[15]

The protective effect of sugars during drying of desiccation-sensitive proteins is based on the glass-forming and interacting properties of the carbohydrate. Sugars replace the hydrogen bonds that exist in aqueous solution during drying,[1] thereby preventing conformational changes of the protein during drying. The long-term stability of proteins in the dried state is determined by both the T_g and the molecular packing.[16,17]

The protective effect of carbohydrates on unilamellar vesicles during drying is based on a narrow balance between the interacting and glass-forming properties of the carbohydrate, and disaccharides seem to be the most effective. The T_g of monosaccharides is generally too low to prevent vesicle fusion during drying, whereas oligo- and polysaccharides are able to prevent fusion, but, due to their large size, are unable to interact with lipid head groups. A direct interaction is pivotal to prevent leakage through the bilayers.[18] Disaccharides are small enough to interact with vesicles and have a sufficiently high T_g to prevent vesicle fusion, which renders them good protectants of vesicles during drying. An interesting exception is the fructan family of oligo- and polysaccharides. Fructans stabilize liposomes against leakage of aqueous content after rehydration progressively more effectively with increasing chain length. Surprisingly, they become less effective in protecting liposomes against membrane fusion with increasing chain length.[19]

In this study, FTIR was used to characterize the hydrogen-bonding network of amorphous carbohydrates of different chain lengths. The OH stretching mode arising from the sugar OH groups was used to establish correlations between the position and width of this band and T_g. In addition, the expansion of hydrogen-bond distances with heating was determined from the temperature shift of the OH stretching band (*WTC*). DSC was used to study the change in heat capacity, ΔC_p, that is associated with the glass transition. The interaction between sugars and POPC vesicles, and that between sugars and poly-L-lysine were studied by monitoring the effect of these biomolecules on the band position of the sugar OH stretching band.

2. Materials and methods

2.1. Sugars

Sucrose, glucose, raffinose, trehalose, and maltose were purchased from Pfahnstiel Laboratories (Waukegan, IL, USA). Dextran-T40 (40 kDa) was obtained from Pharmacia Biotech (Uppsala, Sweden). Glucans **4**, **5**, and **6** were obtained from Megazyme (Wicklow, Ireland). 1-Palmitoyl-2-oleoyl-*sn-glycero*-3-phosphocholine (POPC) was obtained from Avanti Polar Lipids (Alabaster, AL, USA). Poly-L-lysine (57.9 kDa) was obtained from Sigma Chemical Co. (St Louis, MO, USA). Carbohydrate glasses were prepared by rapid air drying of dilute carbohydrate solutions (20 mg/mL) on circular CaF_2 (13×1 mm diameter) IR windows in a cabin continuously purged with dry air (RH <3%). For studies on the effect of 1-palmitoyl-2-oleoyl-*sn-glycero*-3-phosphocholine (POPC) vesicles and poly-L-lysine on hydrogen bonding in dry sugar matrices of different chain lengths, POPC vesicles (20 mg/mL) or poly-L-lysine (57.9 kDa, 20 mg/mL) were added to the carbohydrate solutions at the indicated mass ratios, and the solutions were dried as described above. The POPC–sugar mixtures were sonicated for several minutes, to obtain small unilamellar vesicles of approximately 30 nm in diameter, with the sugar present both on the inside and outside of the vesicles. Residual water in the samples was removed by heating the sample up to 110 °C for approximately 15 min.

2.2. Fourier-transform infrared spectroscopy (FTIR)

Infrared absorption measurements were carried out with a Perkin–Elmer series 1725 or 2000 Fourier-transform infrared spectrometer (Perkin–Elmer, Norwalk, CT), as described previously.[14] The instrument was equipped with a narrow-band mercury/cadmium/telluride LN_2-cooled IR-detector. The temperature of the FTIR cell was regulated by a computer-controlled device, and the temperature of the sample was recorded separately using a thermocouple located very close to the sample windows. The temperature dependence of the FTIR spectra was studied starting with the lowest temperature, with a scanning rate of 1 °C/min. The optical bench was purged with dry CO_2–free air. The acquisition parameters were: 4 cm^{-1} resolution, 32 coadded interferograms, with a 3600–900 cm^{-1} wavenumber range.

Spectral analyses and displays were carried out using the interactive Perkin–Elmer software. The melting of sugar glasses was monitored by observing the position of the OH stretching band (νOH) around 3300 cm^{-1}.

The spectral region between 3600 and 3000 cm^{-1} was selected and normalized. The band position was calculated as the average of the spectral positions at 80% of the total peak height. T_g was determined by linear regression of the wavenumber of the OH stretching band as a function of the temperature in both the liquid and the solid-like regions of the plot. The point of intersection of these two regression lines was defined as the glass transition temperature T_g.[14]

2.3. Differential scanning calorimetry (DSC)

Glass transitions were measured using a Mettler–Toledo DSC822 differential scanning calorimeter (Columbus, OH). Sugar solutions of 50 mg/mL were air dried in a box that was continuously purged with dry air of less than 3% RH. Approximately 5 mg of a sample was transferred in DSC pans, and samples were heated to 110 °C for several h to remove residual water. Samples were scanned at 5 °C/min. Glass transitions were analyzed using the Mettler software.

3. Results

3.1. FTIR spectra of crystalline and amorphous sugars

Figure 1 depicts the IR absorption spectra of amorphous and crystalline trehalose. The IR spectrum of crystalline trehalose is characterized by relatively sharp absorption bands throughout the mid-IR region from 4000 to 900 cm^{-1}, whereas much broader absorption bands are visible in amorphous trehalose. Crystalline trehalose shows the presence of one sharp band around 3500 cm^{-1}, and a few shoulder peaks in the OH stretching region between 3600 and 3000 cm^{-1} that are indicative of hydrogen bonds of defined geometric positions. The broad features of the OH band of amorphous trehalose indicate a wide range of hydrogen-bond lengths and orientations. The main reason for the sharper and more intense peaks in the crystalline state is the higher degree of homogeneity of intermolecular interactions. This leads to less dispersion of vibrational levels and a higher conformational selectivity. Crystallization caused a decrease in νOH_{max}, suggesting an increase in hydrogen-bond density and strength.[20] Six bands can be identified in the C–H stretching region, located between 3000 and 2800 cm^{-1}, of crystalline trehalose, whereas amorphous trehalose shows only one broad band in this region. The H_2O scissoring mode of residual water is shifted from 1685 cm^1 in the crystalline form to 1645 cm^{-1} in the amorphous form, indicating that the water molecules in crystalline trehalose are more strongly hydrogen bonded to the sugar molecules compared to residual water in amorphous trehalose. The bands in the 1500–1200 cm^{-1} region arise mostly from C–H deformation vibrations, and the bands between 1200 and 900 cm^{-1} arise predominantly from a combination of CO (νC–O) stretching and OH bending (δC–O–H) vibrations.[21]

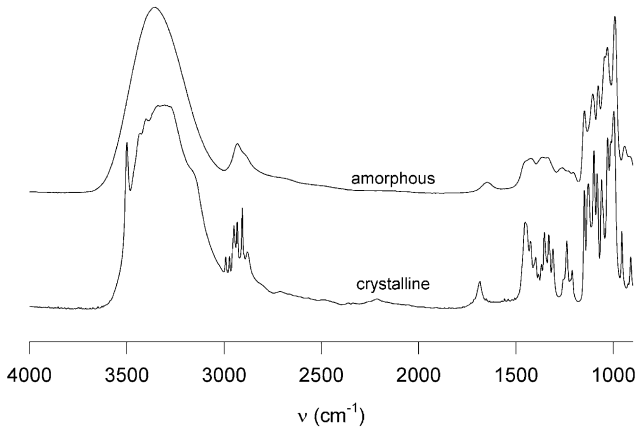

Figure 1. IR spectra of crystalline (lower trace) and amorphous (upper trace) trehalose at 24 °C.

Figure 2 depicts IR spectra of trehalose in solution and at low water content in order to illustrate the effects of dehydration on the spectral region between 1800 and 900 cm^{-1}. As expected, the intensity of the OH scissoring mode of water (at ~1650 cm^{-1}) sharply decreases with decreasing water content. The shape of the region between 1500 and 900 cm^{-1}, however, remains similar during dehydration. The six bands that can be resolved between 1200 and 900 cm^{-1} arise from a combination of νC–O, νC–C, and δC–O–H.[21] The bands at 1150 cm^{-1} (νC–O) and 980 cm^{-1} (νC–O and δC–O–H) have been assigned to the glycosidic linkage. The positions of the bands in the 1200–900 cm^{-1} region progressively shift to a lower wavenumber upon dehydration by approximately 2–4 cm^{-1}, and their bandwidth increases. These dehydration-induced frequency shifts originate from a modification of the level of hydrogen bonding of the C–O–H groups.[21]

We conclude that the shape of the fingerprint region of amorphous trehalose closely resembles that of trehalose in solution and is strikingly different from the fingerprint region of crystalline trehalose. The fact that the IR spectrum of dry amorphous trehalose is similar to the spectrum in solution suggests that the sugar has hydrogen-bonding interactions in the dried state that are comparable to those in the fluid state. Apparently, the hydrogen-bonding interactions between sugar and water in solution are replaced by intermolecular sugar hydrogen bonds upon dehydration.

3.2. Hydrogen bonding in amorphous carbohydrates

Figure 3 depicts the OH stretching mode of various carbohydrates of different molecular weights and T_g's. In all cases, the OH stretching band is a broad band, with

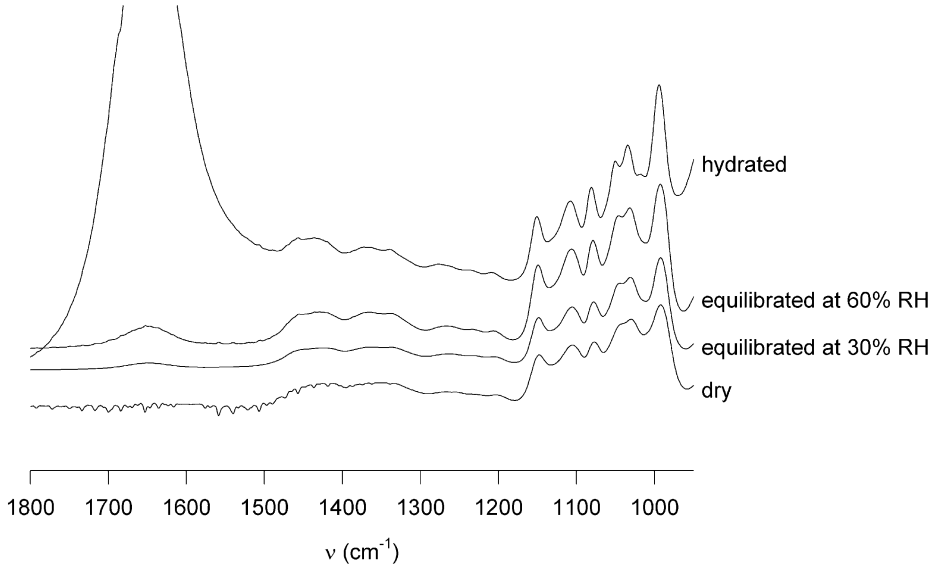

Figure 2. IR spectra of trehalose in solution (200 mg/mL, upper trace), air-dried trehalose equilibrated at 60% RH (third trace), air-dried trehalose equilibrated at 30% RH (water content 3%, second trace), and air-dried trehalose that was heated to 120 °C for 15 min to remove residual water (water content 0%, lowest trace). The spectra were recorded at 24 °C.

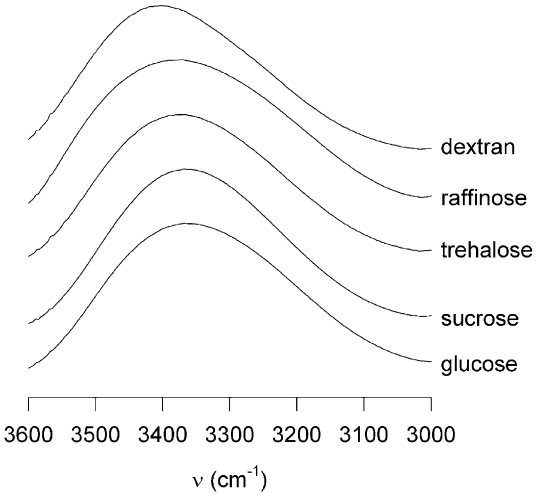

Figure 3. IR region of the OH stretching region of glucose ($T_g = 27$ °C), sucrose ($T_g = 57$ °C), trehalose ($T_g = 108$ °C), raffinose ($T_g = 108$ °C), and dextran ($T_g = 220$ °C), illustrating that the maximum of νOH increases with increasing T_g. All spectra were recorded at 24 °C.

an absorbance maximum at approximately 3350 cm^{-1}. It is evident that the OH band is shifted to higher wavenumber with increasing T_g. Figure 4A shows that there is a positive linear correlation between the band position of the OH stretching mode and the glass transition temperature of the carbohydrate. The wavenumber position of the OH stretching band has been correlated with the geometric parameters of H-bridge formation.[15] Thus, O–H bond lengths and O···O distances can be derived from the spectral positions of the OH band. The positive correlation of νOH with T_g, implies that the average length of the hydrogen bonds increases with increasing T_g.

No correlation was found between the bandwidth of νOH, determined at half intensity, and T_g: the bandwidth ranged from 284 to 341 cm^{-1} (Fig. 4B). This indicates that carbohydrates of different size and T_g have a similar distribution of hydrogen-bond lengths and orientations.

3.3. Thermotropic response of the OH stretching mode

When the band position of the OH stretching vibration band of trehalose is plotted as a function of the temperature, one break in the wavenumber versus temperature plot is observed (Fig. 5). The intersection point at 108 °C is associated with the glass transition of the sugar. The wavenumber–temperature coefficient of νOH, which reflects the thermal expansion of the hydrogen bonds, is a measure for the change in hydrogen-bond strength with temperature.[14] Figure 5 shows that the wavenumber–temperature coefficient of νOH below the glass transition temperature (WTC_g) is smaller than that above T_g (WTC_l). This increase in WTC upon melting of the glass is indicative of an abrupt decrease in hydrogen bonding. The WTC_g values of carbohydrates of different chain lengths and T_g's were determined, in order to establish a correlation between WTC_g and T_g (Fig. 6A). The sugars that were studied include, fructose, octulose, glucose, sucrose, umbelliferose, trehalose, raffinose, glucans (**4**, **5**, and **6**), and dextran-T40. WTC_g increased from approximately 0.10 cm^{-1}/°C in monosaccharides (low T_g) to approximately 0.45 cm^{-1}/°C in

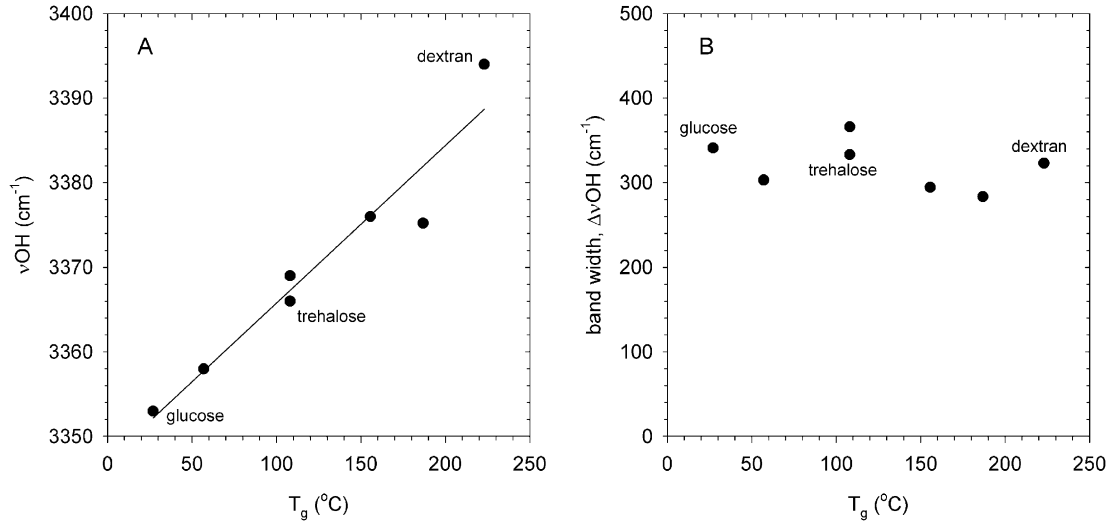

Figure 4. Correlation between band position (A), and bandwidth (B) of the OH stretching mode (at 20 °C) of amorphous carbohydrates and T_g. The linear regression line between νOH and T_g in panel A has an r^2 of 0.93 (a linear regression line between bandwidth and T_g has an r^2 of 0.15). The carbohydrates that were studied include glucose, sucrose, trehalose, raffinose, glucan (**4** and **6**), and dextran. All measurements were done at 24 °C.

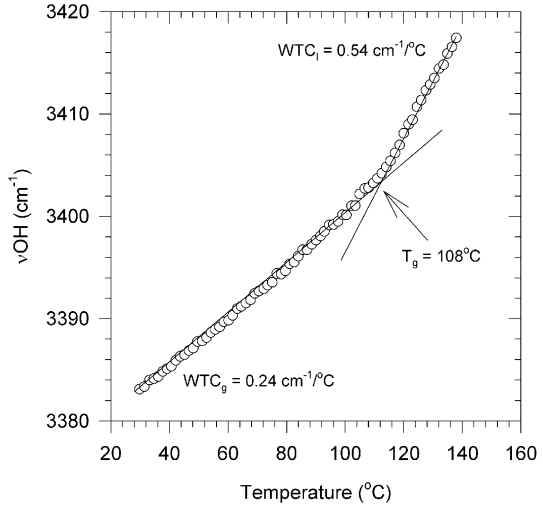

Figure 5. Wavenumber versus temperature plot of amorphous trehalose. The intersection between the linear regression lines in the glassy and liquid state denotes the glass transition temperature. The glass transition temperature, T_g, and the wavenumber–temperature coefficients in the glassy (WTC_g) and liquid (WTC_l) state are indicated in the figure.

polysaccharides (high T_g). The increase in WTC_g with increasing T_g denotes a decrease in average strength of hydrogen bonding. The *WTC* after melting of the glass, WTC_l did not show a clear correlation with T_g and ranged from 0.48 to 0.60 $cm^{-1}/°C$ for the carbohydrates that were tested (Fig. 6B). Thus, ΔWTC, the difference between WTC_l and WTC_g decreases with increasing T_g, which implies that carbohydrates with a high T_g exhibit lesser rearrangements in hydrogen bonding upon melting of the glass compared to sugars with a low T_g.

3.4. DSC measurements of carbohydrate glasses

We investigated whether the correlations between *WTC* and T_g that were derived from the FTIR studies coincided with differences in ΔC_p of the sugars, as measured by DSC. DSC has been extensively used to study glass transitions of carbohydrates.[10,22,23] The glass transition from the glassy to the rubbery state can be measured using DSC as a change in heat capacity, ΔC_p, upon melting of the glass. Figure 7 shows that ΔC_p decreases with increasing T_g. Figure 8 shows that there is a negative linear correlation between ΔC_p and WTC_g ($r^2 = 0.94$). This implies that the change in heat capacity during the transition from the glassy to the rubbery state is associated with the strength of the hydrogen-bonding network in the glassy state. A stronger hydrogen-bonding network in the glassy state correlates with a greater ΔC_p.

3.5. Interaction between carbohydrates and macromolecules

In order to obtain insight in the stabilization of macromolecules by sugars the interaction between sugars and POPC vesicles, and that between sugars and poly-L-lysine was studied by monitoring the effect of these biomolecules on the band position of the sugar OH stretching band.

The effect of poly-L-lysine on the band position of the OH stretching mode of glucose, sucrose, trehalose, and dextran, is shown in Figure 9. The decrease in wavenumber position of the OH stretching band with increasing sugar–polypeptide ratio are indicative of a decrease in hydrogen-bond distances upon introduction

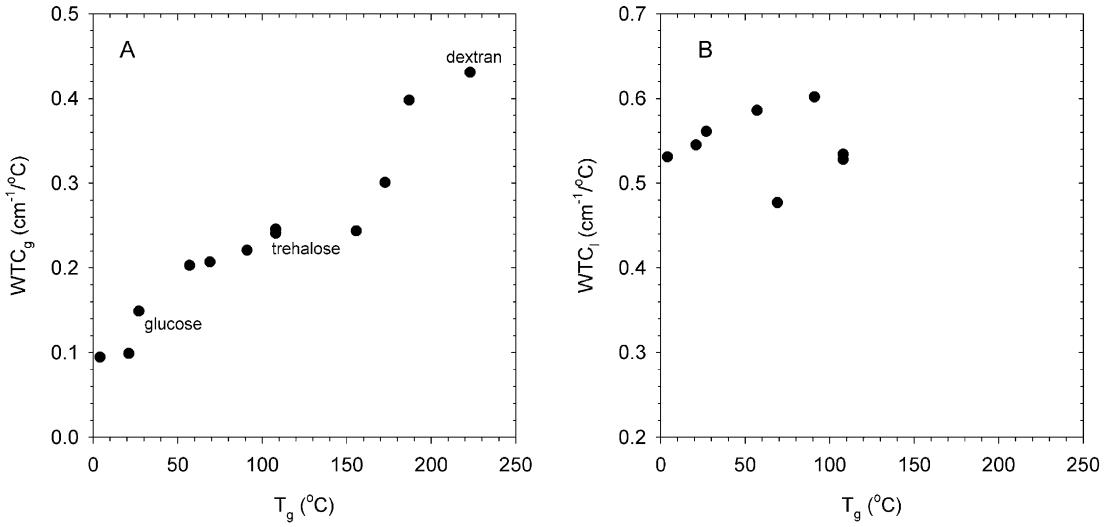

Figure 6. Correlation between WTC_g (A), and WTC_l (B) of amorphous carbohydrates and T_g. The carbohydrates that were studied include glucose, octulose, sucrose, umbelliferose, trehalose, raffinose, glucan (**4**, **5**, and **6**), and dextran-T40. Data are partly taken from Wolkers et al.[14]

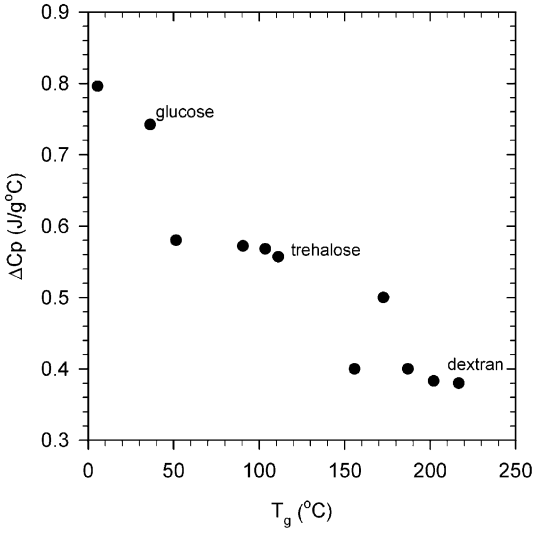

Figure 7. Plot of the change in heat capacity upon melting of the glass, ΔC_p, of various carbohydrates as a function of T_g (filled circles). The glass transition temperature and ΔC_p were measured using DSC. The carbohydrates that were studied include fructose, glucose, sucrose, maltose, trehalose, raffinose, glucan (**4**, **5**, and **6**), and dextran (T10 and T40).

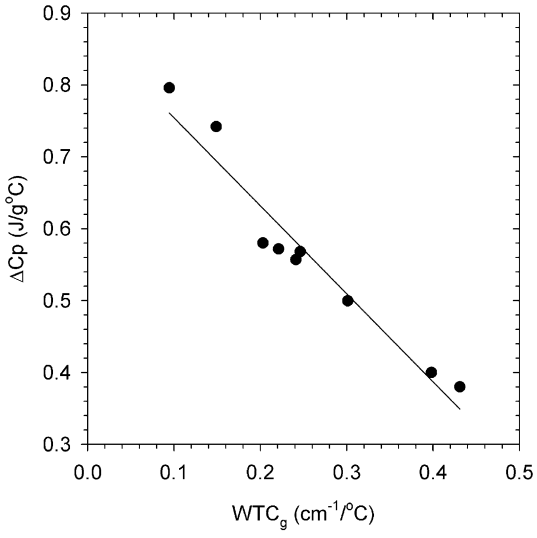

Figure 8. Correlation plot between WTC_g and ΔC_p. The linear regression line $\Delta C_p = -1.22 \times WTC_g + 0.88$ has an r^2 of 0.94.

of the polypeptide. Poly-L-lysine was used because it lacks OH groups and therefore has minimal interference with the OH band arising from the sugars.[24] Introduction of poly-L-lysine decreased the band position of the OH stretching vibration in all cases. This indicates that carbohydrates and polypeptides interact through hydrogen bonding, which results in a decrease of the average length of the hydrogen bonds in the sugar matrix. At a polypeptide–sugar mass ratio of 3 (excess protein), the wavenumber of the OH stretching mode ranged from 3310 to 3298 cm^{-1} for the different sugars, indicating that there are only minor differences in the average length of the sugar–polypeptide hydrogen bonds.

A similar study was conducted to determine if these sugars also interact with vesicles in the dried state. Figure 10 shows that introduction of POPC vesicles in amorphous glucose, sucrose, and trehalose decreased the band position of the OH stretching band, indicating a decrease in the average length of the hydrogen bonds. The *v*OH of these sugars plateaus to approximately 3300 cm^{-1} at lipid–sugar ratios greater than 1. The *v*OH of dextran, however, is hardly affected in the presence of the vesicles, which indicates that dextran shows minimal

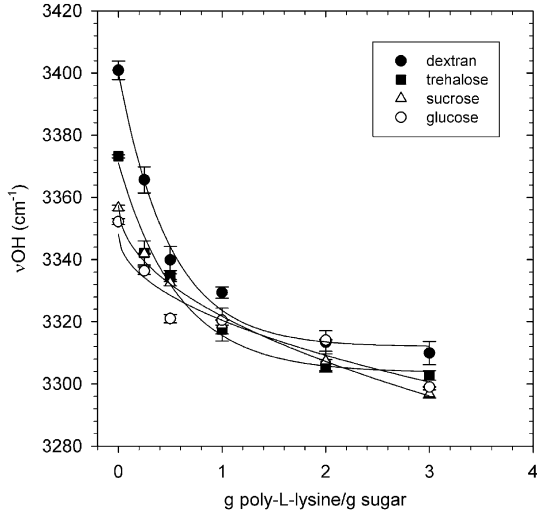

Figure 9. Effect of poly-L-lysine on the band position of the OH stretching band (νOH) of amorphous glucose, sucrose, trehalose, and dextran-T40. All measurements were done at 24 °C. The data are means of three experiments, and the error bars reflect the standard error.

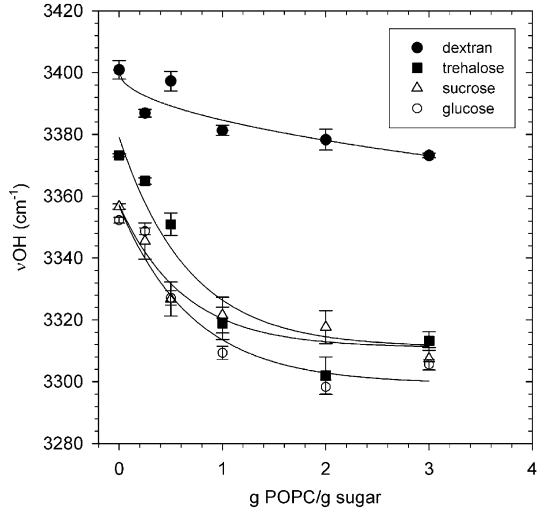

Figure 10. Effect of small unilamellar POPC vesicles on νOH of amorphous glucose, sucrose, trehalose, and dextran-T40. All measurements were done at 24 °C. The data are means of three experiments, and the error bars reflect the standard error.

interaction with POPC vesicles through hydrogen bonding.

We conclude that dextran and poly-L-lysine interact through hydrogen bonding, whereas dextran and POPC vesicles show only minimal interaction. The latter is most likely due to geometric restrictions preventing full interaction between polysaccharides and lipid bilayers. Crowe and co-workers[18] have shown that polysaccharides are able to prevent fusion of vesicles during drying, but that they are unable to prevent leakage of the vesicle's content. By contrast, disaccharides are known to be effective stabilizers of vesicles during drying.[1] FTIR studies have shown that the protection of vesicles by disaccharides is in part due to depression of the phase transition temperature by these sugars in the dried state.[18] Interestingly, the geometric constraints that prevent interaction between vesicles and dextran, do not occur between dextran and poly-L-lysine. The polypeptide compensates for the loss of hydrogen bonding with water in solution by formation of hydrogen bonds with the carbohydrates.[24] In contrast to the interaction between POPC and carbohydrates, the interaction between polypeptides and sugars through hydrogen bonding appears not to be limited by size.

4. Discussion

We have used FTIR to obtain information on the hydrogen-bonding network of amorphous sugars of different sizes and T_g. FTIR provides unique information on the molecular structure and intermolecular interactions that exist in these materials that cannot be obtained by other methods. The positive correlation that was found between νOH and T_g indicates that the average length of the hydrogen bonds in amorphous sugars increases with increasing T_g. We have also shown that introduction of polypeptides or vesicles in amorphous carbohydrate matrices result in a decrease of the average length of hydrogen bonding, which shows that sugars and these macromolecules interact through hydrogen bonding. The studies on the thermotropic response of the νOH of carbohydrates, shows that sugars exhibit a greater degree of freedom to rearrange hydrogen bonds with increasing T_g. The increase in the thermal expansion of hydrogen bonds in the glassy state (WTC_g) with increasing T_g is correlated with a decrease in ΔC_p of the glass transition.

The glass transition temperature of carbohydrates varies with molecular weight, in a predictable manner;[10] T_g generally increases with increasing molecular weight. However, it appears difficult to predict the T_g of disaccharides based solely on molecular weight. The glass transition temperatures of dry sucrose and maltose, for example, are 70 and 95 °C,[22] respectively, whereas the T_g of trehalose is 110 °C.[4] The latter falls in the same range as the T_g of oligosaccharides such as raffinose and stachyose, which are reported to be 106 and 123 °C, respectively.[11] The wide range of T_gs in disaccharides, are likely due to differences in molecular packing, which as we show here, may be associated with differences in intermolecular hydrogen bonding. Differences in hydrogen bonding, and hence in the molecular packing of the amorphous carbohydrates, are reflected in the band position, and thermotropic response of νOH. The differences in WTC_g between sucrose and trehalose (0.20 and 0.24 cm^{-1}/°C, respectively), for example, suggest that trehalose is more loosely packed than sucrose,

which may explain the large difference in T_g between these sugars. The more loose structure of high T_g carbohydrate glasses that is demonstrated here, has also been suggested on the basis of EPR experiments.[25] The rotational mobility in the glassy state was shown to increase with increasing T_g.[11] Also the molecular free volume at T_g increases with increasing molecular weight for small polymers/oligomers,[26] and the average radius of molecular free volume holes at T_g was found to increase with T_g.[27,28] Thus, high T_g oligo- and polysaccharides will form a glassy matrix with a higher molecular free volume, which allows for more rearrangements in hydrogen bonding during temperature changes.

Molecular movements become abruptly prevented below T_g and the configurational modes are frozen abruptly. Thus changes in enthalpy, volume, and entropy occur more slowly below T_g than above T_g.[23] Here we show that the glass transition is manifested as an abrupt decrease in the rotational freedom of hydrogen bonds below T_g. We suggest that the decrease in the thermotropic response of hydrogen bonds below T_g is associated with a decrease in entropy. The increase in WTC_g with increasing T_g indicates that sugars with a high T_g undergo greater rearrangements in hydrogen bonding during temperature changes than sugars with a low T_g. This indicates that carbohydrate glasses with a higher T_g are more loosely packed and undergo greater changes in entropy with changes in temperature. This more loose molecular packing increases the configurational modes of hydrogen bonding, which stabilizes the glassy state. WTC_l was found to be the same for all carbohydrates tested, which indicates that once carbohydrate glasses are melted, they exhibit a similar expansion of hydrogen-bond distances with heating. Thus, ΔWTC, the difference between WTC_l and WTC_g, decreases with increasing T_g. Interestingly, the increase in WTC_g with increasing T_g was found to be correlated with a decrease in ΔC_p. Thus the change in heat capacity during the glass transition is directly correlated with the strength of the hydrogen-bonding network in the glassy state. Both ΔC_p and the abrupt increase in WTC at T_g reflect that changes in entropy occur more rapidly above T_g than below T_g.

We suggest that WTC_g is a measure for the degree of order, or entropy in the glassy state. It reflects the molecular packing of the sugars in the glassy state. Thus, we propose that a higher degree of freedom to rearrange the molecular packing during temperature changes stabilizes the glassy state.

5. Conclusions

We conclude that the differences in T_g between carbohydrates of various sizes are associated with differences in strength and density of hydrogen bonds. We demonstrated that the band position of the OH stretching mode exhibits a positive linear correlation with T_g. The bandwidth, however, did not show a correlation with T_g. We have shown that introduction of poly-L-lysine in amorphous sugars decreased the average length of the hydrogen bonds in the dry matrix, irrespective of the size of the carbohydrate. POPC vesicles were found to decrease the average length of the hydrogen bonds of low molecular weight sugars, but the hydrogen-bonding network of dextran was minimally affected by the POPC vesicles. Thus, the interaction between sugars and POPC vesicles is limited by the size of the carbohydrate, whereas the interaction between sugars and poly-L-lysine is not. The FTIR studies on the thermotropic response of νOH show that the average strength of hydrogen bonding decreases with increasing T_g. The latter shows a direct correlation with a decrease in ΔC_p of the glass transition. High T_g sugars exhibit a greater degree of freedom to rearrange hydrogen bonds during changes in temperature than low T_g sugars. We suggest that this higher degree of freedom to rearrange the molecular packing during temperature changes stabilizes the amorphous state.

Acknowledgements

The glucans that were used in this study were a kind gift of Dr. Dirk Hincha. This project was financially supported by grants HL57810 and HL61204 from NIH, and 981711 from DARPA.

References

1. Crowe, J. H.; Crowe, L. M.; Oliver, A. E.; Tsvetkova, N. M.; Wolkers, W. F.; Tablin, F. *Cryobiology* **2001**, *43*, 89–105.
2. Horbowicz, M.; Obendorf, R. L. *Seed Sci. Res.* **1994**, *4*, 385–406.
3. Crowe, J. H.; Carpenter, J. F.; Crowe, L. M.; Anchordoguy, T. J. *Cryobiology* **1990**, *27*, 219–231.
4. Crowe, L. M.; Reid, D. S.; Crowe, J. H. *Biophys. J.* **1996**, *71*, 2087–2093.
5. Crowe, L. M.; Womersley, C.; Crowe, J. H.; Reid, D.; Appel, L.; Rudolf, A. *Biochim. Biophys. Acta* **1986**, *861*, 131–140.
6. Prestrelski, S. J.; Tedeschi, N.; Arakawa, T.; Carpenter, J. F. *Biophys. J.* **1993**, *65*, 661–671.
7. Guo, N.; Puhlev, I.; Brown, D. R.; Mansbridge, J.; Levine, F. *Nat. Biotechnol.* **2000**, *18*, 168–171.
8. Gordon, S. L.; Oppenheimer, S. R.; Mackay, A. M.; Brunnabend, J.; Puhlev, I.; Levine, F. *Cryobiology* **2001**, *43*, 182–187.
9. Wolkers, W. F.; Walker, N. J.; Tablin, F.; Crowe, J. H. *Cryobiology* **2001**, *42*, 79–87.
10. Slade, L.; Levine, H. *Crit. Rev. Food Sci. Nutri.* **1991**, *30*, 115–360.
11. Buitink, J.; van den Dries, I. J.; Hoekstra, F. A.; Alberda, M.; Hemminga, M. A. *Biophys. J.* **2000**, *79*, 1119–1128.
12. van den Dries, I. J.; van Duschoten, D.; Hemminga, M. A. *J. Phys. Chem.* **1998**, *102*, 10483–10489.

13. Ludescher, R. D.; Shah, N. K.; McCaul, C. P.; Simon, K. V. *Food Hydrocolloids* **2001**, *15*, 331–339.
14. Wolkers, W. F.; Oldenhof, H.; Alberda, M.; Hoekstra, F. A. *Biochim. Biophys. Acta* **1998**, *1379*, 83–96.
15. Lutz, E. T. G.; Van der Maas, J. H. *J. Mol. Struct.* **1994**, *324*, 123–132.
16. Davidson, P.; Sun, W. Q. *Pharm. Res.* **2001**, *18*, 474–479.
17. Sun, W. Q.; Davidson, P. *Biochim. Biophys. Acta* **1998**, *1425*, 235–244.
18. Crowe, J. H.; Oliver, A. E.; Hoekstra, F. A.; Crowe, L. M. *Cryobiology* **1997**, *35*, 20–30.
19. Hincha, D. K.; Zuther, E.; Hellwege, E. M.; Heyer, A. G. *Glycobiology* **2002**, *12*, 103–110.
20. Ottenhof, M.; MacNaughtan, W.; Farhat, I. A. *Carbohydr. Res.* **2003**, *338*, 2195–2202.
21. Kacurakova, M.; Mathlouthi, M. *Carbohydr. Res.* **1996**, *284*, 145–157.
22. Orford, P. D.; Parker, R.; Ring, S. G. *Carbohydr. Res.* **1990**, *196*, 11–18.
23. Roos, Y. H. *Phase Transitions in Foods*; Academic: London, 1995; pp 1–360.
24. Wolkers, W. F.; van Kilsdonk, M. G.; Hoekstra, F. A. *Biochim. Biophys. Acta* **1998**, *1425*, 127–136.
25. Dzuba, S. A.; Golovina, E. A.; Tsvetkov, Y. D. *J. Magn. Reson. Ser. B* **1993**, *101*, 134–138.
26. Fox, T. G.; Loshaek, S. *J. Polym. Sci.* **1955**, *15*, 371–390.
27. Bartos, J. *Colloid Polym. Sci.* **1996**, *274*, 14–19.
28. Li, H. L.; Ujihara, Y.; Nanasawa, A.; Jean, Y. J. *Polymer* **1999**, *40*, 349–355.